available at www.sciencedirect.com

ScienceDirect

journal homepage: www.elsevier.com/locate/agrformet

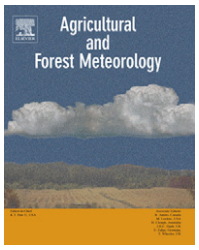

Estimating energy balance fluxes above a boreal forest from radiometric temperature observations

J.M. Sánchez [a,*], V. Caselles [a], R. Niclòs [a], C. Coll [a], W.P. Kustas [b]

[a] Earth Physics and Thermodynamics Department, University of Valencia, C/Dr. Moliner, 50, 46100 Burjassot, Spain
[b] Hydrology and Remote Sensing Laboratory, USDA-ARS, Bldg. 007, BARC West, Beltsville, MD 20705, United States

ARTICLE INFO

Article history:
Received 7 February 2008
Received in revised form
29 October 2008
Accepted 30 December 2008

Keywords:
STSEB model
Energy fluxes
Boreal forest
Energy balance closure
Canopy temperature

ABSTRACT

The great areal extent of boreal forests confers these ecosystems potential to impact on the global surface-atmosphere energy exchange. A modelling approach, based on a simplified two-source energy balance model, was proposed to estimate energy balance fluxes above boreal forests using thermal infrared measurements. Half-hourly data from the Solar-Induced Fluorescence Experiment, carried out in a Finnish boreal forest, was used to evaluate the performance of the model. Energy balance closure, determined by linear regression, found all fluxes to underestimate available energy by 9% ($r^2 = 0.94$). Significance in the energy balance of the heat storage in the air and in the soil terms was also analyzed. Canopy temperatures, measured by a CIMEL Electronique CE 312 radiometer, together with ancillary meteorological variables and vegetation characteristics, were used to run the model. Comparison with ground measurements showed errors lower than ± 15 W m^{-2} for the retrieval of net radiation, soil heat flux and storage heat flux, and about ± 50 W m^{-2} for the sensible and latent heat fluxes. A sensitivity analysis of the approach to typical operational uncertainties in the required inputs was conducted showing the necessity of accurate measurements of the target radiometric surface temperature.

1. Introduction

An increasing number of studies on energy and mass exchange between forests and the atmosphere have been conducted over the past few years, in order to understand both forest functioning and the role of forests as sinks or sources of atmospheric pollutants.

In particular, the boreal forest is the major biome occupying the circumpolar region between 50° and 70° north. Boreal forest's great areal extent (11% of the terrestrial surface) and its unique biophysical properties confer these ecosystems potential to impact on the Earth's climate. The remote location and harsh climate of boreal forests kept them elusive to first studies on energy exchange and energy balance. Advances in infrastructures and technology allowed subsequent inclusion of these ecosystems in the scientific community focus (Lindroth, 1985; Lafreur, 1992; Baldocchi and Vogel, 1996). The BOReal Ecosystem-Atmosphere Study (BOREAS), a large-scale international experiment in the northern boreal forests of Canada, is one of the most remarkable efforts to improve our understanding of the boreal forest interactions with the atmosphere. Two extensive field campaigns in 1994 and 1996 put over 300 scientists and aircrew into the field (Sellers et al., 1995, 1997; Baldocchi et al., 1997). A current network of eddy-covariance (EC) towers measuring long-term carbon and energy fluxes in contrasting ecosystems and climates (FLUXNET, http://www.fluxnet.ornl.gov/fluxnet/index.cfm) contains an increasing number of boreal forest sites. In this work we will focus on one of these sites: Sodankylä, Finland. An intensive field campaign, the Solar-Induced Fluorescence

* Corresponding author. Tel.: +34 963543249; fax: +34 963543385.
E-mail address: Juan.M.Sanchez@uv.es (J.M. Sánchez).
0168-1923/$ – see front matter
doi:10.1016/j.agrformet.2008.12.009

Experiment-2002 (SIFLEX-2002, Davidson et al., 2002), was carried out in this boreal forest area from April to June 2002, collecting all the data required for the present study. In general, conifer forests have a greater ability to exchange mass and energy with the atmosphere than other vegetation types (Baldocchi et al., 1997). For example, they are optically darker than broad-leaved forests and short vegetation (Sellers et al., 1995). This attribute allows them to absorb more solar radiation and gives them greater potential to evaporate water and heat the air and soil. Conifer forests are also aerodynamically rougher than broad-leaved forests, shrubs, and herbaceous vegetation. This characteristic enhances their ability to transfer mass and energy with the atmosphere (Shuttleworth, 1989). One important difference between the forests and other vegetation surfaces is the presence of an understorey, which contributes to the overall exchange of mass and energy. Until recently, forest-atmosphere exchanges have often been modelled using a "big-leaf" approach. However, comparisons between different sites may lead to erroneous interpretations if existing differences between their understoreys are not taken into account (Lamaud et al., 1996). For this reason, a two-source energy balance model is required to account for the energy exchange from the canopy and the understorey vegetation. The main objective of this work is to test the recently proposed Simplified Two-Source Energy Balance (STSEB) model (Sánchez et al., 2008a), based on the Norman et al. (1995) model, over the conditions of the boreal forest. Unfortunately, energy fluxes below the forest canopy were not registered during the SIFLEX experiment. This paper is exclusively focused on the energy exchange above the forest canopy.

The surface energy balance can be conveniently expressed as

$$R_n = H + LE + G + S + Q \quad (1)$$

where R_n is the net radiation flux (W m^{-2}), H is the sensible heat flux (W m^{-2}), G is the soil heat flux (W m^{-2}), S is the storage heat flux (W m^{-2}), and Q represents other minor terms such as photosynthesis, (W m^{-2}). Typically, Q is neglected from Eq. (1). The importance of S is expected to be small in short canopies with minimal biomass; however this term must be maintained for tall, forested sites (McCaughey, 1985). Historically, energy balance closure has been accepted as an important test of eddy-covariance data. A general concern has been developed within the micrometeorological community because surface energy fluxes ($LE + H$) are frequently underestimated by the EC method by about 10–30% relative to estimates of available energy (R_n–G–S) (Wilson et al., 2002; Twine et al., 2000; Stannard et al., 1994). An energy imbalance has implications on how energy flux measurements should be interpreted and how these estimates should be compared with model simulations. An additional objective of this work is to analyze the energy balance closure over the boreal forest conditions.

Although there are several surface-based methods that can accurately measure surface heat fluxes at point locations, it is not feasible to use a network of these systems to create spatially distributed flux maps because of the high variability of real landscapes. Micrometeorological approaches can only realistically provide measurements representative of a particular type of vegetation cover when there is a reasonably extensive, uniform area of that vegetation immediately upwind of the instruments. The use of satellite remote sensing techniques supplies the frequent lack of ground-measured variables and parameters required for estimating surface energy fluxes over large areas. As shown in Sánchez et al. (2008b) these surface variables and parameters can be extracted from the combination of the multi-spectral information contained in a satellite image. Also, vegetation parameters can be assigned using a satellite-based land uses map. The key issue is establishing, at different scales, relationships that link remote sensing observations to the variables needed to formulate surface fluxes (Njoku et al., 1996). In two-source energy balance models, soil and canopy temperatures are key inputs. The main limitation of these approaches based on remote sensing data is that reliable measurements of the soil and canopy temperatures are not readily available from most satellite systems. However, some authors have proposed models to obtain soil and canopy temperatures from dual-angle radiometric temperatures (François, 2002). Jia et al. (2003) developed an algorithm to retrieve these temperature components from the previous version of the Advanced Along-Track Scanning Radiometer (AATSR) on board ENVISAT satellite. Different equations have been proposed to evaluate required surface variables such as albedo (Russell et al., 1997) and emissivity (Valor and Caselles, 1996). The incoming long-wave radiation can be determined by introducing humidity and temperature profiles through the atmosphere (Brutsaert, 1982) in a radiative transfer code. This parameter shows a relatively spatial homogeneity at a regional scale which allows the use of local radiosoundings (Sánchez et al., 2008b), even though these profiles can be obtained from instruments such as the Atmospheric Infrared Sounder (AIRS) on board EOS-Aqua (Chachine et al., 2001). However, nearly all approaches require some supplementary local meteorological and/or surface information (Moran et al., 1997). The air temperature and wind speed data, needed in the STSEB model, must be measured at local meteorological stations and then interpolated over the large area, if required, which is an additional limitation to the practical use of the model with remote sensing data. The uncertainties due to the monitoring of the main STSEB model inputs, lead to errors in the estimated fluxes. A sensitivity analysis is performed to quantify the effect of these large-scale input uncertainties. This information is useful to evaluate the practical use of the model in application with satellite data in the conditions of a boreal forest ecosystem.

This paper is organized as follows: Section 2 describes the experimental site and measurements. The modelling approach, as well as the scheme to estimate the component temperatures required, are shown in Section 3. The results of surface energy fluxes are compared with ground measurements in Section 4. A study of the energy balance closure in the boreal forest, as well as the sensitivity analysis of the model to uncertainties in key inputs, is also provided in this section. Finally, the main conclusions of this work are given in Section 5.

2. Site description and experimental setup

2.1. Site description

This work was carried out as part of the SIFLEX-2002 project. The measurement campaign was performed at Sodankylä, in a

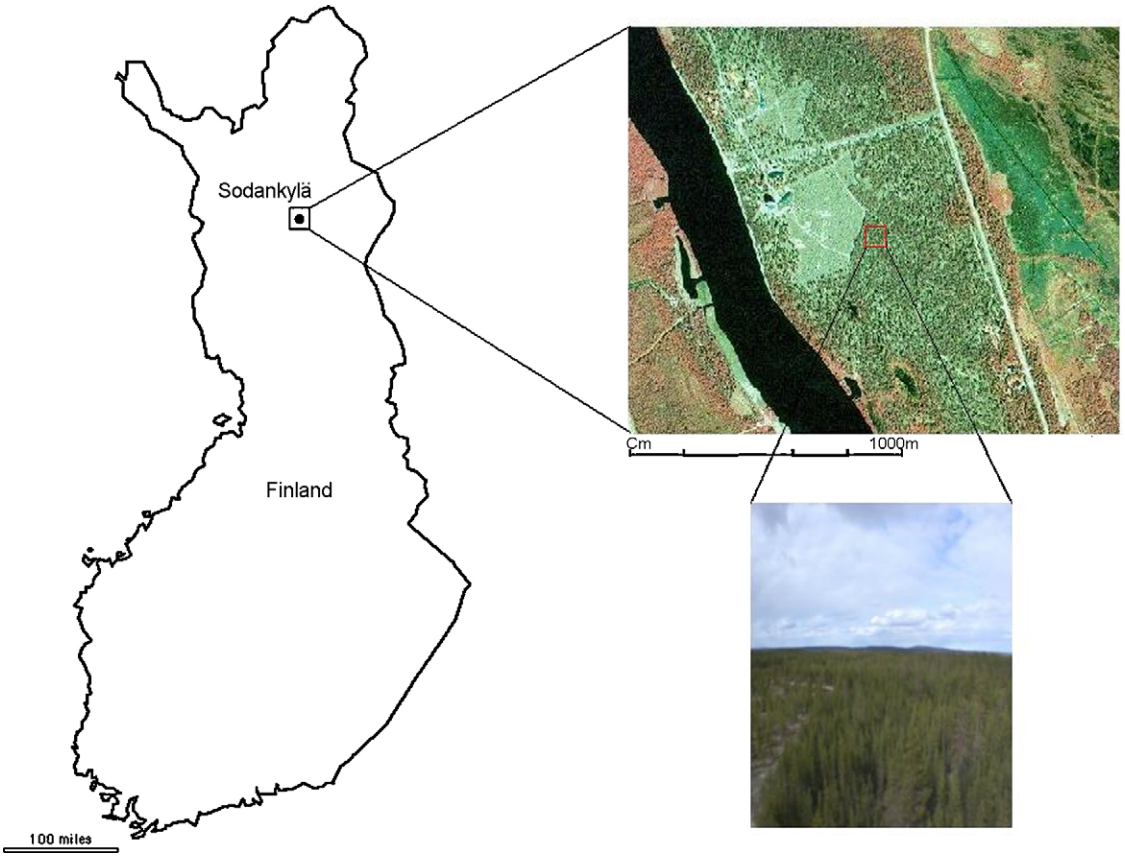

Fig. 1 – Location and target view of the boreal forest site in Sodankylä, Finland, where the SIFLEX-2002 campaign was carried out.

northern boreal forest area of Finland (Fig. 1) from April to June of 2002. The study area was placed at the Artic Research Center, Finnish Meteorological Institute (FMI) (67°21′42.7″N, 26°38′16.2″E, 179 m above sea level), 100 km north of the Artic Circle. Sodankylä site belongs to the Coordinated Enhanced Observing Period (CEOP) reference sites of the Global Energy and Water Cycle Experiment (GEWEX) of the World Climate Research Programme, and to the CO_2 flux station network of the CARBOEUROPE project.

This site is representative for the northern edge of the boreal zone. Winters normally have temperatures well below freezing with permanent snow and soil frost. This is a boreal forest area, with pines (*Pinus sylvestris* L.) of more than 10 m in height and 100 years old in average, and a tree density of about 2100 trunks per ha. The soil type is fluvial sandy podzol where lichens, cowberry and crowberry are common (see Table 1).

2.2. *Measurements*

During the SIFLEX-2002 campaign, solar radiation and surface radiometric temperature measurements were carried out by the University of Valencia. The FMI was in charge of measuring the *LAI* (Leaf Area Index), the meteorological variables and the surface energy fluxes that will be used in this work (Davidson et al., 2002).

The meteorological variables were obtained from a 48-m height micrometeorological mast placed in the site. Air temperature and humidity were measured at different levels with a Vaisala HMP 45 sensor, with accuracies of ±0.2 °C and ±1%, respectively. Wind speed data was collected by a Vaisala WAA252 anemometer, with an accuracy of ±0.1 m/s, placed at a height of 23 m. Other weather parameters such as the fraction of cloud cover or the cloud height were measured manually at the FMI-Artic Research Centre. Besides, atmospheric

Table 1 – Canopy and soil parameters of the boreal forest in Sodankylä, Finland.

Forest parameter	Value
Tree specie	*Pinus sylvestris* L.
Tree density	2100 trees ha^{-1}
Soil type	Fluvial sandy podzol
Understorey vegetation	Lichens, cowberry and crowberry
Average tree height	11 m
Reference height	23 m
LAI	1.37
Clumping factor (nadir)	0.84
Vegetation coverage (nadir)	0.44
Effective surface albedo	0.11
Emissivity (canopy)	0.978
Emissivity (soil)	0.953
Effective surface emissivity	0.976
Volumetric soil moisture range	3–15%

radiosoundings (Vaisala RS-80) of temperature, humidity and wind were launched twice a day at the study site.

LAI measurements were made twice during the campaign at 12 points distributed around the study site. It was measured using a LICOR LAI-2000, which calculates the leaf area from radiation measurements taken with an optical sensor having a field of view of 148°. A time series of soil and canopy albedo values was also registered during the campaign.

Canopy temperature values were inferred using thermal radiance measurements of pine trees performed every 10 min by a multi-channel thermal infrared radiometer CIMEL ELECTRONIQUE CE 312. The CIMEL was placed on a tower observing the target from a height of 12 m. The observation angle was fixed at 85° from nadir, using a quasi-horizontal path to assure a homogeneous view of the canopy and to avoid the observation of the soil (Niclòs et al., 2005). Effect of possible pointing errors was checked by changing the observation angle slightly, and the thermal spatial variability around the target was negligible. This radiometer has four spectral channels: one broadband, 8–14 μm (band 1), and three narrow channels. Channel 3 (10.5–11.5 μm) was used in this experiment (Legrand et al., 2000). Samples of pine branches and understorey vegetation covering the soil below the trees were collected to measure their emissivity by means of the CE-312 radiometer using the Box Method (Rubio et al., 1997, 2003). The effective surface emissivity of the target was estimated according to the method proposed by Valor and Caselles (1996) (see Appendix A) from the canopy and soil corresponding values (Table 1). Radiosounding data for several days with different atmospheric conditions were introduced into the MODTRAN 4 code (Berk et al., 1999) to get estimates of the atmospheric parameters required to correct the brightness temperatures of atmospheric effects.

Sensible and latent heat fluxes were measured by the FMI with a SATI-3Sx sonic anemometer and a LICOR-7000 analyzer using eddy-covariance methodology with an uncertainty in flux estimation of ±15–20% (Brutsaert, 1982; Aurela et al., 2001). Measurements were taken at 23 m in height. Fluxes were corrected for frequency response limitation and finite averaging period. Note that there are factors that tend to limit the overall performance of the EC system. These factors lengthen the effective response time of the EC system leasing to a flux loss. By estimating this effect for the different frequencies of the flux spectrum, we can correct for the underestimated flux. The flux values were corrected taking a reference co-spectrum as described in Massman and Lee (2002). At low frequencies, the method of the recursive mean filter is used with the 30-min averaging period (Baldocchi, 2003). Global and reflected short-wave radiation was measured by a Kipp&Zonen CM11 sensor, and the incoming and outgoing long-wave components were registered by an Eppley Precision infrared radiometer. Net radiation was measured by a REBS Q-7 sensor. All these sensors were mounted at 46 m height. Also, the effective albedo value of the target was obtained from the aforementioned incoming and reflected short-wave radiation measurements (Table 1). Soil heat flux was measured by a single HFT3 soil heat flux plate at a depth of 7 cm. Soil temperature was measured at 2, 5, 10, 20, 50, and 100 cm depth by using a set of thermocouples, and volumetric soil moisture at 5, 10, 20, 30, and 50 cm through Delta-T TDR-probes. The heat stored in the soil profile above the plate, computed from the temporal change in soil temperature and soil water content, was also considered. Finally, the heat storage in the air profile from the surface to the eddy instruments was also obtained from observed air temperature values at the three levels considered in this experiment (3, 18, and 23 m). According to Finnigan (2006) there is an underestimation in the storage term when the averaging time used is long compared with a short integral timescale. However, the reader should note that in the case of the boreal forest the effect of S in the global energy balance is minor compared with the rest of the fluxes. The averaging time for all data was 30 min.

Although the field campaign was conducted from April to June of 2002, this analysis is based on the data taken from the 5th of May in order to avoid additional complexities due to snow cover.

3. Modelling approach

3.1. Surface energy flux estimates

3.1.1. Sensible heat flux

The Simplified Two-Source Energy Balance (STSEB) model has been recently proposed by Sánchez et al. (2008a). The STSEB approach is based on a patch representation of the energy exchange from soil (understorey vegetation in this case) and canopy with the atmosphere. As a difference with the two-layer models, no direct coupling is allowed between soil and vegetation. According to this configuration, the addition between the soil and canopy contributions to the total sensible heat flux, H, must be weighted by their respective partial areas as follows:

$$H = P_v H_c + (1 - P_v) H_s \tag{2}$$

where P_v is the canopy cover fraction at nadir, and the subscripts c and s refer to the canopy and soil components, respectively.

In Eq. (2), H_s and H_c are expressed as

$$H_c = \rho C_p \frac{T_c - T_a}{r_a^h} \tag{3a}$$

$$H_s = \rho C_p \frac{T_s - T_a}{r_a^a + r_a^s} \tag{3b}$$

where ρC_p is the volumetric heat capacity of air (J K^{-1} m^{-3}), T_a is the air temperature at a reference height (K), T_c and T_s are the canopy temperature and the soil temperature, respectively (K), r_a^h is the aerodynamic resistance to heat transfer between the canopy and the reference height (s m^{-1}), r_a^a is the aerodynamic resistance to heat transfer between the point $z_0 + d$ (z_0: roughness length, d: displacement height) and the reference height (s m^{-1}), r_a^s is the aerodynamic resistance to heat flow in the boundary layer immediately above the soil surface (s m^{-1}). (For details about the expressions to estimate these resistances see Appendix A). The height $z_0 + d$ is considered as the reference point at which energy exchanges soil-vegetation-atmosphere are produced. Air temperature at this reference height is called aerodynamic temperature, and it

Table 2 – Summary of the main model inputs and parameters together with the instruments used to be measured or the equations required to be estimated.

Model inputs/ parameters	Measured/parameterised
T_a	Vaisala HMP 45 sensor
u	Vaisala WAA252 anemometer
LAI	LICOR LAI-2000
h	Manually
T_c	CIMEL CE-312 infrared radiometer
R_g Reflected short-wave radiation	Kipp&Zonen CM11 radiometer
L_{sky} Outgoing long-wave radiation	Eppley precision infrared radiometer
ε_s	Box Method
ε_c	
ε	Eq. (A9)
α	Derived from R_g and Reflected short-wave radiation
T_R	Inferred from outgoing long-wave radiation
T_s	Derived from T_R and T_c values, and Eq. (7)
r_a^h	Eq. (A1)
r_a^a	Eq. (A2)
r_a^s	Eq. (A3)
$P_v(\theta)$	Eq. (A10)

represents the temperature of the air layer in contact with both the vegetation and the soil. Assuming that the air temperature does not change significantly from the soil surface boundary layer to the level $d + z_0$, and the thickness of the air layer below the level $d + z_0$ is typically much shorter than that above, r_a^a accounts for the resistance effect of the total air layer below the reference height (Table 2).

3.1.2. Net radiation

Net radiation R_n provides the available radiative energy to be allocated between the terms shown in Eq. (1). In the current study, the net radiation is expressed as:

$$R_n = (1-\alpha)R_g + \varepsilon L_{sky} - \varepsilon\sigma T_R^4 \quad (4)$$

where R_g is the solar global radiation (W m^{-2}), L_{sky} is the incident long-wave radiation (W m^{-2}), α is the surface albedo, ε is the effective surface emissivity, σ is the Stefan-Boltzmann constant, and T_R is the effective radiometric surface temperature (Table 2).

3.1.3. Soil heat flux

Commonly, G is parameterised as a constant proportion of R_n that is fixed for the entire day or period of interest. Recommended values range typically from 0.15 to 0.40 in the literature (Choudhury et al., 1987; Humes et al., 1994; Kustas and Goodrich, 1994). Many empirical studies have shown that G is neither constant nor negligible on diurnal timescales. Field observations show that G/R_n can range from 0.05 to 0.50 depending on the time of day and surface conditions (Kustas et al., 1993). In this study, we used the simple function derived by Santanello and Friedl (2003) applied to the boreal forest conditions:

$$\frac{G}{R_n} = A\cos\left[\frac{2\pi t}{B}\right] \quad (5)$$

where t is time in seconds relative to 10 a.m. in this case (note that t is not absolute time). Parameters A and B, were estimated using the empirical relationships between them and the amplitude of diurnal variation in surface temperature obtained by Santanello and Friedl (2003). In this study, these parameters resulted $A = 0.20$, and $B = 90950$ s. Using data from different experimental campaigns, Santanello and Friedl (2003) showed that B ranges from 75,000 to 142,000 s depending on different factors. Also, these authors observed, from a set of simulations, that a variation of ±15,000 s in the value of B has no significant influence in the results of G/R_n.

Note that a single heat flux plate was set up due to experimental limitations when it is known that a battery of them is necessary to extract firm conclusions about the soil heat flux estimates. However, the FLUXNET data suggests that inaccuracies in G have a lower impact on energy balance closure in forests than in agricultural, chaparral and grassland sites (Wilson et al., 2002).

3.1.4. Storage heat flux

Wilson et al. (2002) showed that including S in the regressions of $H + LE$ against R_n–G–S in forests, the slope increased by an average of 7%. Therefore, the storage heat flux cannot be neglected on an hourly basis as it is usually done on a daily basis (Baldocchi et al., 1997). The sensible heat storage flux in the surface-air space is usually calculated as an addition of the rate of change of the air temperature at several levels in the surface-air layer multiplied by the volumetric heat capacity of the air (McCaughey, 1985). Air column information is then required for a precise estimate of S. Since the working of this method is quite limited, we suggest a method for estimating the storage term when no proper measurements are available, which is a common situation given the number of sensors required for such a estimation:

$$S = \rho C_p \frac{\Delta T_c}{\Delta t} z \quad (6)$$

where T_c is assumed as a first approximation of the air temperature at the height of the canopy top, when these data are not available, and z is the reference height from which sensible and latent heat fluxes were measured.

Oliphant et al. (2004) compared the results of S obtained using a complete temperature profile with those using a single temperature measurement in a temperate deciduous forest. These authors showed good agreement coming when using the value of the single temperature measured at half the height at which turbulent fluxes were measured. In our case, this level matches just the tree top.

Oliphant et al. (2004) showed that the values of the biomass heat storage flux were rarely over 10 W m^{-2}, and thus too small to justify a more intensive effort for its estimate and modelling. However, recent papers such as Haverd et al. (2007)

and Gu et al. (2007) showed that this term may range from −50 to 50 W m^{-2} or even more, being then a substantial part of the surface energy budget. Unfortunately, the precise measurements of internal stem temperatures required to calculate this biomass heat storage flux were not available in the SIFLEX campaign.

Providing that R_n, H, G, and S are obtained using the aforementioned formulations, latent heat flux LE can be derived as the residual term of the energy balance equation.

3.2. Surface temperature components

The value of the effective radiometric surface temperature at a viewing angle θ, $T_R(\theta)$ (K), is related to the fraction of the target occupied by soil versus vegetation, but also to the emissivity values of both components:

$$\varepsilon T_R{}^4(\theta) = P_v(\theta)\varepsilon_c T_c^4 + (1 - P_v(\theta))\varepsilon_s T_s^4 \quad (7)$$

where ε_s and ε_c are soil and canopy emissivities, respectively. The angular vegetation cover fraction $P_v(\theta)$ can be estimated from measurements of LAI (see Appendix A).

Note that T_c and T_s are assumed to represent spatially weighted averages of the sunlit and shaded portions of the canopy and soil, respectively. Even though it is well-known that soil emissivity may be lower than canopy emissivity, and also that the cavity effect tends to increase the value of ε under conditions of partial vegetation cover, many authors have used equation (7) with the assumption that $\varepsilon = \varepsilon_c = \varepsilon_s$. This simplification may yield significant differences in the retrieval of the component temperatures from dual-angle observation of $T_R(\theta)$ for example. Also note that Eq. (7) is based on the Stefan-Boltzmann law, and thus the emissivity values correspond to broadband (3–30 μm) whereas field thermal radiometers usually work in narrower bands. Also, typical libraries (Salisbury and D'Aria, 1992 or Snyder et al., 1997) span only between 3.3 and 14.0 μm, while significant long-wave radiation extends to approximately 30 μm. However, some works have dealt with the evaluation of the difference between the narrow band and the broadband emissivity, such as that of Ogawa et al. (2002). These authors analyzed the spectra of the Arizona State University emission spectral library and showed good agreement between the narrow (8–14 μm) and the broadband emissivity. A root mean square difference (RMSD) of 0.02 was obtained for the whole set of samples analyzed.

As stated in Sánchez et al. (2008a), the main limitation of the STSEB model is that reliable values of the component temperatures are required. This can be achieved with two different viewing angle measurements of the effective temperature over the target (François, 2002; Merlin and Chehbouni, 2004). In this case, special care must be taken with the emplacement of the radiometers in the experimental setup, in order to make sure that both instruments are viewing exactly the same portion of the target, and that the differences in the radiometric temperatures registered are only due to change in the viewing angle. These experimental problems, especially remarkable in forest ecosystems, can be avoided if T_R is registered at a single viewing angle, and direct measurements of only one, T_c or T_s, are also available. The other temperature component can be inferred using Eq. (7). Furthermore, the left-hand term in Eq. (7) corresponds to the outgoing long-wave radiation divided by the Stefan-Boltzmann constant (Brutsaert, 1982). Therefore, measurements of this variable can substitute the T_R measurements taken by a thermal radiometer. Unfortunately, T_s measurements were not registered in this experiment. Thus, T_R values inferred from the measurements of outgoing long-wave radiation, as mentioned above, together with measurements of T_c, were used in this work to retrieve T_s, required in Eq. (3b). The strategy used to determine T_c from ground thermal infrared radiance, measured by the CIMEL CE-312 radiometer, under variable cloudiness conditions, was described in Niclòs et al. (2005).

4. Results and discussion

4.1. Energy balance closure

Some authors such as Lamaud et al. (2001), Wilson et al. (2002), and Foken et al. (2006) discussed possible causes for the lack of energy balance. However, the problem of this energy imbalance remains unconcluded.

In this work energy balance closure was evaluated for the 2-month dataset. Data were rejected when wind speed was lower than 1 m s^{-1} so as to assure a correct working of the sonic instrumentation. Linear regression coefficients (slope and intercept) were derived from the ordinary least squares relationship between the half-hourly measurements of the available energy (R_n) against the addition of the rest of the terms considered in the energy balance equation in this work ($H + LE + G + S$). A slope of 0.91 and an intercept of −1.9 W m^{-2} were observed. The coefficient of determination (r^2) resulted 0.94. Baldocchi et al. (1997) obtained, for a Canadian boreal forest dataset, a slope equal to 0.94, an intercept of −8 W m^{-2}, and a coefficient of determination equal to 0.94. Gustafsson et al. (2003) observed that the sum of turbulent heat fluxes and the soil heat flux constituted in average 86% of the observed net radiation, using data from a boreal forest zone belonging to the NOPEX (Northern Hemisphere Climate-Processes Land-Surface Experiment) experimental site in Sweden. Wilson et al. (2002) reported values of slopes and intercepts ranging from 0.53 to 0.99, and from −33 to 37 W m^{-2}, respectively. The coefficients of determination ranged from 0.64 to 0.96 for the 22 FLUXNET sites studied.

4.2. Surface energy fluxes retrieval

The performance of the proposed approach was assessed by considering the daytime data collected during the experiment. Daytime flux statistics are more descriptive of overall model utility since nighttime flux estimates are constrained to be near zero.

For estimating net radiation, Eq. (4) was applied using the ground-measured values of R_g and L_{sky}. T_R values were extracted from the ground-measured values of outgoing long-wave radiation as indicated in Section 3.2. Fig. 2a shows the results of modelled versus measured values (net radiation sensor) of R_n. A quantitative analysis of this regression is shown in Table 3. An overestimation of 3 W m^{-2}, and a RMSD

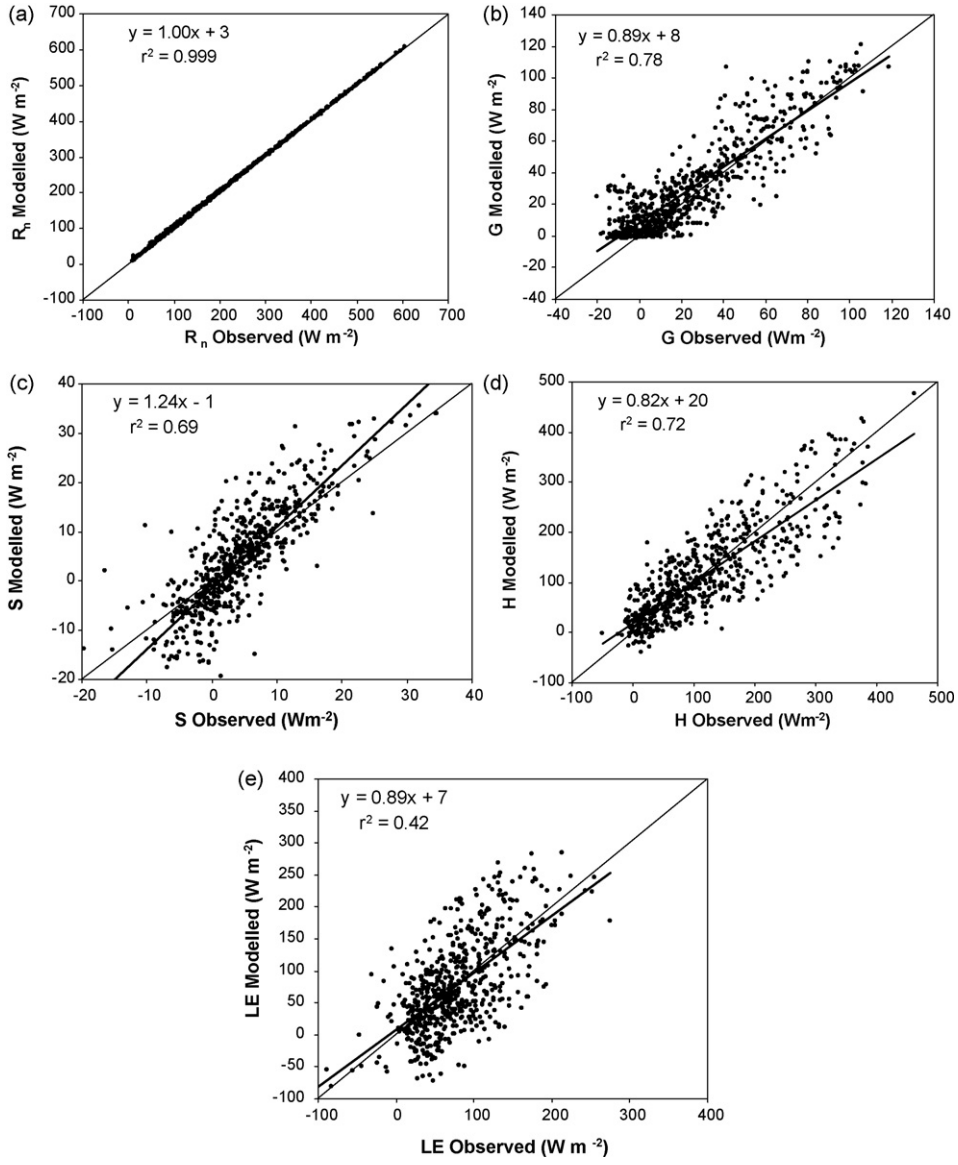

Fig. 2 – Linear regressions between the surface energy fluxes estimated versus their corresponding ground measured values: (a) R_n, (b) G, (c) S, (d) H (eddy-covariance measurements) and (e) LE (residual technique applied).

of ± 4 W m^{-2} are observed in the total R_n for the campaign data. Regarding the soil heat flux, G, an overestimation of 6 W m^{-2}, and a RMSD of ± 15 W m^{-2} for the whole period were obtained (Fig. 2b). Note that this should not be considered as an independent model test since G was parameterised. The storage heat flux, S, was modelled using Eq. (6). A negligible biased estimator of -0.3 W m^{-2} was calculated, with a RMSD of ± 7 W m^{-2} (Fig. 2c).

Table 3 lists statistics comparing turbulent fluxes estimates of H and LE with the eddy-covariance fluxes in their original form (EC), and corrected for closure using the residual (RE) and Bowen ratio (BR) techniques (Twine et al., 2000). In the RE method, the direct eddy-covariance measurements of H are assumed reliable and lack of closure is largely due to an undermeasurement of LE. In the BR method, it is assumed both turbulent fluxes are under measured with the amount distributed between H and LE based on the Bowen ratio (H/LE), which defines the fraction of available energy going into sensible versus latent heat.

Model comparisons with H_{EC} and LE_{RE} are shown in Fig. 2d and e. After retrieving T_s values from equation (7), and correcting the aerodynamic resistances for atmospheric stability/instability (Sánchez et al., 2008a), H was estimated via Eqs. (2), (3a), and (3b). Comparison between modelled and measured H shows a negative bias of -2 W m^{-2}, and a RMSD of ± 50 W m^{-2} (Fig. 2d).

For LE obtained as a residual term from Eq. (1), there is a clear tendency to overestimate the observed latent heat flux, LE_{EC}, with a slope of 1.10 and RMSD = ± 70 W m^{-2}. When the RE closure technique is applied to the eddy observations, the slope of the linear regression decreases to 0.89 and the RMSD decreases by 20 W m^{-2} (Fig. 2e). If energy closure is enforced by the Bowen ratio technique (LE_{BR}) the slope increases more than 30%, and RMSD = ± 60 W m^{-2} is now obtained (see Table 3).

Table 3 – Statistical analysis of the proposed model performance with the daytime SIFLEX-2002 dataset. H_{EC} and H_{BR} are the sensible heat fluxes estimated by eddy-correlation and Bowen ratio, respectively. LE_{EC}, LE_{RE} and LE_{BR} are the latent heat fluxes measured by eddy-correlation, and obtained using residual method and Bowen ratio method as closure, respectively.

Flux	BIAS[a] (W m^{-2})	RMSD[b] (W m^{-2})	MAD[c] (W m^{-2})	a[d]	b[e] (W m^{-2})	r^2[f]
R_n	+3	±4	±3	1.00	3	0.999
G	+6	±15	±11	0.89	8	0.777
S	0	±7	±5	1.24	−1	0.693
H_{EC}	−2	±50	±40	0.82	20	0.715
H_{BR}	−17	±60	±50	0.74	17	0.671
LE_{EC}	+23	±70	±50	1.10	18	0.234
LE_{RE}	−1	±50	±40	0.89	7	0.418
LE_{BR}	+15	±60	±50	1.31	−5	0.352

[a] Biased estimator: BIAS $= \sum_{i=1}^{n}(P_i - O_i)/n$.
[b] Root mean square difference: RMSD $= \left[\sum_{i=1}^{n}(P_i - O_i)/n\right]^{1/2}$.
[c] Mean absolute difference: MAD $= \sum_{i=1}^{n}|P_i - O_i|/n$.
[d] Slope of the linear regression: $P_i = aO_i + b$.
[e] Intercept of the linear regression: $P_i = aO_i + b$.
[f] Coefficient of determination, where P_i and O_i are the predicted and observed variables, respectively.

Therefore, for the data studied here, the RE closure technique, using H_{EC} and assigning all imbalance error to LE (LE_{RE}), yields the best agreement between modelled and measured turbulent fluxes. These findings support the theory of an under-measurement problem with the eddy-covariance system together with the LICOR-7000 analyzer affecting only the latent heat flux. Other possible causes of observed energy imbalances, such as length of the sampling interval or the heterogeneity of the landscape, seem to have no significant effect according to the negligible bias shown by the modelled H when compared with the corresponding EC measurements. Recent works have also found optimal agreement using the RE method (Sánchez et al., 2008a; Li et al., 2005). However, there is no firm consensus yet on how to resolve the energy imbalance with eddy-covariance, and no firm conclusion can be extracted from our findings either, further investigation is required.

An example of the performance of the model is shown in Fig. 3. Modelled and measured fluxes are plotted together for a period of 8 days (from 28 May to 4 June). The first 4 days are completely cloud-free, whereas variable cloudiness conditions occurred during the last 4 days. Reasonable good agreement is observed between measured and modelled fluxes also under cloudy skies. In fact, these deviations are more evident under cloud-free conditions. This might be due to the temperature differences between the sunlit and shaded portions of the canopy and soil since, as mentioned above, T_c observations and T_s estimations were assumed to represent weighted averages of both sunlit and shaded areas. A plot has been included in Fig. 3 showing H_s and H_c separately. We can observe that the main contribution to the total sensible heat flux of the target comes from the canopy whereas the underestorey contribution is minor but not negligible. Unfortunately, these results cannot be tested at this time since H_s and H_c were not measured separately in this experiment.

Few studies have dealt with the simulation of surface energy fluxes in boreal forests, and those which have, used to base the modelling on daily averages. On a hourly or half-hourly basis, weaker performance has been always observed. Gustafsson et al. (2003) assessed the performance of the land surface scheme used in the European Centre for Medium-Range Weather Forecast (ECMWF) in a boreal forest located in the NOPEX experimental site (Sweden). Traits of this forest were different to those in the SIFLEX site, with Scots pines of around 25-m height and LAI values from 3 to 5. Linear regressions between simulated versus observed surface fluxes, based on daily averages, showed slopes of 0.90, 2.39, 0.73, and 0.80 for R_n, G, H, and LE, respectively. RMSD values ranged between ±10 and ±30 W m^{-2} for all fluxes. Wu et al. (2001) used data from the BOREAS experiment to compare results from two-layer and single-layer canopy models with Lagrangian and K-theory approaches. Trees in this boreal aspen forest were 21-m tall and maximum LAI values were 2.3. Comparison of modelled and measured daytime average values of LE above the forest showed RMSD values of ±40 W m^{-1} for the single-layer model, ±50 W m^{-2} for K-theory two-layer model and ±40 W m^{-2} for the Lagrangian two-layer model. The same forest was used by Grant et al. (2006) to test five models included in the Fluxnet-Canada Research Network (FCRN). Regressions of simulated on observed hourly averaged fluxes showed slopes ranging from 0.70 to 1.30, and RMSD values from ±20 to ±60 W m^{-2}, depending on the model, for the sensible and latent heat fluxes. Sánchez et al. (2007) have recently used the SIFLEX dataset to elaborate and explore the applicability of a semi-empirical method with MODIS satellite data. Comparison between modelled and ground-measured fluxes showed RMSD values of about ±60 W m^{-2} at an instantaneous scale, whereas at a daily-average scale RMSD values decreased below ±30 W m^{-2}.

Sánchez et al. (2008a) tested the STSEB model over maize using radiometric soil and canopy temperature direct observations. For that, data from one summer growing season was used. Note that the STSEB version used in that paper neglected the storage heat flux term. Also a constant proportion of the net radiation, fixed for the entire day and period of interest, was used to estimate the soil heat flux in the maize. RMSD values of about ±20, ±40, ±20, and ±50 W m^{-2} were obtained

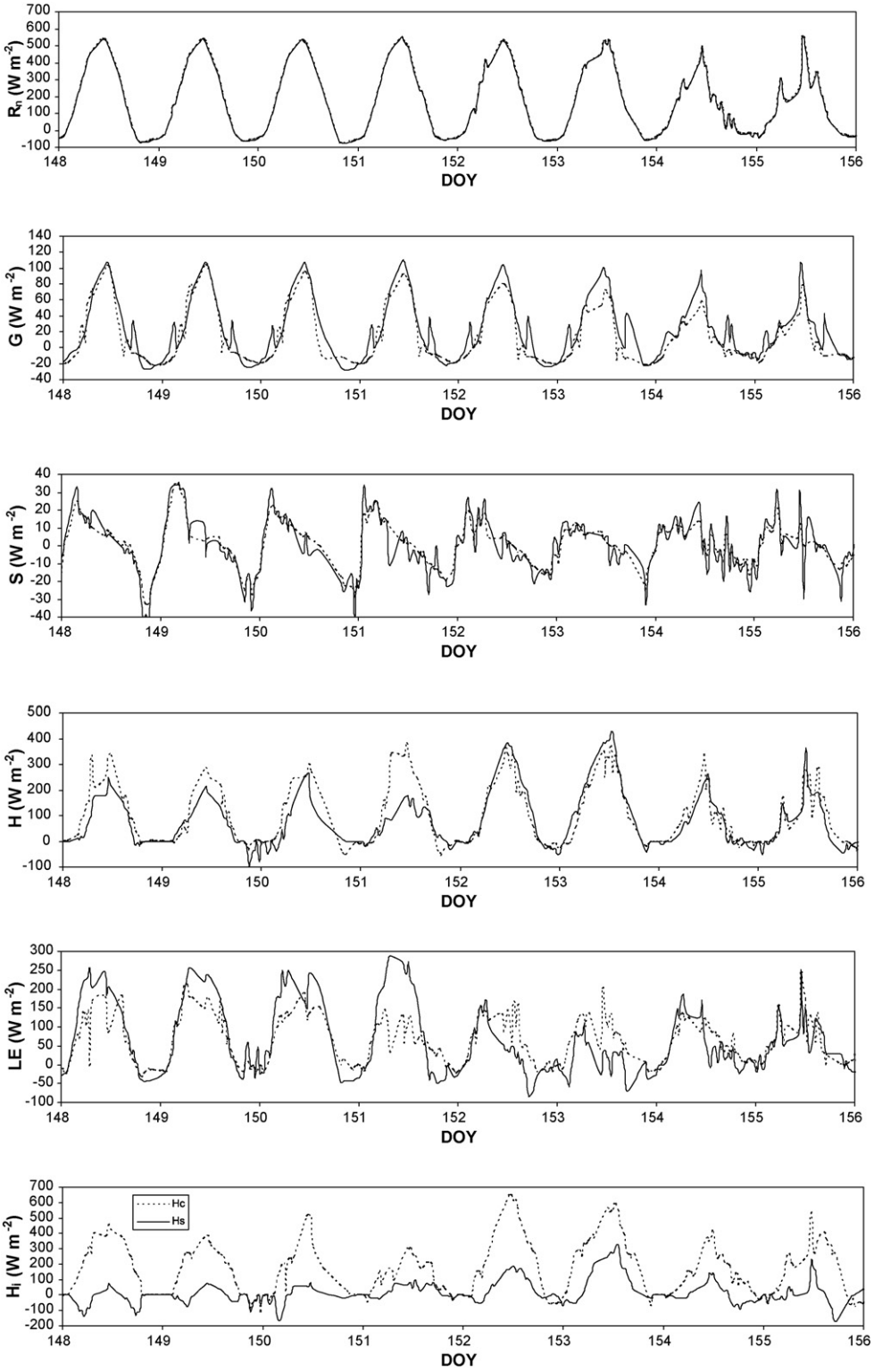

Fig. 3 – Times series of measured (dotted line) and estimated (continuous line) surface energy fluxes for the period from May 28 to June 4, in order from the top: R_n, G, S, H, and LE. The bottom plot shows the evolution of H_s and H_c for the same time period.

for R_n, G, H, and LE, respectively. Comparing these results with those obtained in the boreal forest, it is observed that the error in G estimations is reduced when introducing the Santanello and Friedl (2003) function in the model. Average error value in LE estimation in the boreal forest is of the same order as in the maize crop, while the estimation error in H is significantly higher in the boreal forest than in the maize. However, differences between the two sites in the available energy and its partitioning among all the fluxes must be taken into account at this point. Overall, G values are lower in the boreal

Table 4 – Average values of the relative sensitivity, S_p, of the model to the uncertainties, X, in the required inputs, p, for estimating H, R_n, and LE (H_0 = 208 W m^{-2}, R_{n0} = 385 W m^{-2}, LE_0 = 100 W m^{-2}). These uncertainties correspond to typical errors expected for operational monitoring over extensive boreal forest areas.

Input	T_c (°C)	T_R (°C)	T_a (°C)	u (m s^{-1})	R_g (W m^{-2})	L_{sky} (W m^{-2})	LAI	Ω_0	h (m)	α	ε_c	ε_s
P_0	14.3	13.7	11.0	4.0	499	314	1.37	0.84	11	0.11	0.978	0.953
X	1 °C	1 °C	0.5 °C	0.5 ms^{-1}	5%	5%	20%	20%	10%	20%	0.01	0.01
H	0.15	0.48	0.32	0.18	0.0019	0.0013	0.04	0.04	0.14	$<10^{-3}$	0.17	0.22
R_n	0	0.03	0	0	0.12	0.08	0.008	0.008	0	0.06	0.009	0.011
LE	0.32	1.08	0.67	0.37	0.36	0.25	0.06	0.06	0.30	0.18	0.33	0.41

forest than in the maize. More significant is the difference in terms of the turbulent fluxes. For the maize crop, maximum values of H and LE reached about 200 and 500 W m^{-2}, respectively, whereas in the boreal forest these values were about 400 and 200 W m^{-2}, respectively. Therefore, the energy exchange between the surface and the atmosphere is dominated by the evapotranspiration in the maize, while in the boreal forest the energy transference is basically controlled by the sensible heat flux.

Average values of H and LE in a range of 4 h around solar midday, for the present campaign, were close to 200 and 100 W m^{-2}, respectively. According to these values, an error of ±50 W m^{-2} yields a relative estimation error of ±25% in terms of H, and ±50% in terms of LE.

4.3. *Sensitivity analysis*

The uncertainties in the inputs for the proposed model may lead to significant uncertainties in the estimated fluxes. A sensitivity analysis was performed for the current experience following the method suggested by Zhan et al. (1996). According to these authors the relative sensitivity, S_p, of a model flux estimate, Z, to X uncertainties in a parameter p, can be expressed as

$$S_p(X) = \left| \frac{Z_- - Z_+}{Z_0} \right| \quad (8)$$

where Z_0, Z_+, and Z_- are the fluxes (H, R_n, or LE) predicted when p equals its reference value p_0, when p_0 is increased by X, and when p_0 is decreased by X, respectively, with all other input parameters held constant at their reference values. For this study, average values of the inputs were considered as reference, corresponding to a range of 4 h around solar midday. A list of all the inputs required by the model, as well as their average values and assigned uncertainties, is shown in Table 4. These uncertainties correspond to typical errors expected for operational monitoring over extensive boreal forest areas, assuming horizontal homogeneity, according to the methodology described. Sensitivity results are also listed in Table 4. Effective radiometric surface temperature and air temperature have the greatest impact on H, showing relative sensitivity values above 25%. Net radiation is mainly affected by R_g and L_{sky} inputs, but always showing sensitivity values below 15% for the uncertainties considered. Similar sensitivity results were obtained by Sánchez et al. (2008a) using the maize dataset. The main difference lies in the T_c input. The model is shown to be much less sensitive to the canopy temperature under the boreal forest conditions. Special care must be taken with T_R since an uncertainty of 1 °C may lead to an error of almost 50% in H. Note that this type of sensitivity analysis does not address multiple input uncertainties that might cause cumulative errors, but also may tend to cancel out reducing the overall error in the flux estimates. Also note that sensitivities associated with the local validation experiment reported in previous section are lower than those expected for remotely driven experiments, since typical errors associated with input values measured locally, using infrared radiometers and local meteorological towers, are lower too. The highest sensitivity values in LE estimate were also obtained for T_R and T_a inputs. However, relative sensitivity of the model output in LE to assumed uncertainties in most of the inputs exceeded 30%. This is due to the fact that under the conditions of the boreal forest much of the available energy was converted to sensible heat flux, as mentioned before. As a result, the sensitivity of the model output in LE to uncertainty in T_R even exceeded 100% of its reference value. This may represent a considerable obstacle to estimate instantaneous latent heat fluxes in boreal forest ecosystems using this method unless very accurate T_R data are available. However, the retrieval of the rest of the terms of the energy balance equation is feasible.

5. Conclusions

The purpose of this paper was to test the recently proposed STSEB model (Sánchez et al., 2008a) under conditions different to those of the maize crop in which it was firstly validated. A boreal forest ecosystem was selected because of its potential to impact the global energy exchange. This paper is based on the SIFLEX-2002 experimental campaign carried out in a FLUXNET site in Sodankylä, Finland, during the spring of 2002. Meteorological variables and fluxes were measured along with the radiometric temperature of pine trees.

An expression to estimate the storage heat flux in the air from canopy temperature data was introduced in the STSEB scheme. Also, the equation used to estimate the soil heat flux was adapted to account for the diurnal variation of its ratio with the net radiation since it was proved to reproduce better results. A technique to retrieve radiometric soil temperature information (when not directly available), from canopy temperature and outgoing long-wave radiation, was proposed and applied in this work.

The energy balance closure was evaluated. An under-estimation of the available energy of 9% has been shown, with a coefficient of determination equal to 0.94, when all fluxes were considered. Results obtained suggest that this imbalance might be due to under-estimation in the measure of LE. Errors lower than ±15 W m^{-2} for the retrieval of net radiation, soil heat flux

and storage heat flux, and about ±50 W m^{-2} for the sensible and latent heat fluxes, were obtained considering half-hourly daytime data. Using directly measured H values and assigning all imbalance errors to LE yield the best agreement between modelled and measured turbulent fluxes. These results are in agreement with the scarce studies on modelling surface fluxes in boreal forests. Resolving the two components of the sensible heat flux informs us that the main contribution to the total sensible heat flux of the target comes from the canopy whereas the understorey contribution is minor but not negligible.

The operational use of the model in application with remote sensing data was explored by means of an analysis of the sensitivity of the model flux output to uncertainties in the required inputs. The air temperature and specially the effective radiometric surface temperature were shown to have the greatest impact on the model estimates. Comparing these results in the boreal forest with those obtained by Sánchez et al. (2008a) in the maize crop, lower sensitivities are generally obtained in the H estimate in the boreal forest. However, relative errors in the LE retrieval are significantly higher in the boreal forest as a consequence of the low values of LE registered in this ecosystem. This may represent a considerable obstacle to estimate instantaneous latent heat fluxes in boreal forest ecosystems using this method unless very accurate T_R data are available. As for the rest of the terms of the energy balance equation, results reinforce the utility of the STSEB model shown in Sánchez et al. (2008a) in a maize crop, now under the conditions of a boreal forest, where the sensible heat flux represents a significantly greater proportion of the available energy. Further field experiments and modelling studies are required to continue testing the model over different landscapes.

Acknowledgements

This work was funded by the *Ministerio de Educación y Ciencia* (Projects CGL2004-06099-C03-01 and CGL2007-64666_CLI, co-financed with European Union FEDER funds, *Acciones Complementarias* CGL2005-24207-E/CLI and CGL2006-27067-E/CLI, and *Juan de la Cierva* Research Grant of Dr. Niclòs), and the University of Valencia (*V Segles* Research Grant of Mr. J.M. Sánchez). The valuable remarks and suggestions of Dr. E. Valor (University of Valencia), Dr. M.C. Anderson (HydroLab, USDA-ARS), and Dr. T. Laurila (Finnish Meteorological Institute) are also appreciated.

Appendix A. Summary of equations to estimate model parameters

The aerodynamic resistances r_a^h, r_a^a, and r_a^s are expressed as follows:

$$r_a^h = \frac{[Ln((z_u - d)/z_{0M}) - \Psi_M((z_u - d)/L) + \Psi_M(z_{0M}/L)]}{[Ln((z_T - d)/z_{0H}) - \Psi_H((z_T - d)/L) + \Psi_H(z_{0H}/L)]} \frac{}{k^2 u} \quad \text{(A1)}$$

$$r_a^a = \frac{[Ln((z_u - d)/z_{0M}) - \Psi_M][Ln((z_u - d)/z_{0M}) - \Psi_H]}{k^2 u} \quad \text{(A2)}$$

$$r_a^s = \frac{1}{0.0025(T_s - T_c)^{1/3} + 0.024u_s} \quad \text{(A3)}$$

where z_u and z_T are the measurement heights (m) for wind speed, u (m s^{-1}), and air temperature, respectively, d is displacement height (m), z_{0M} is the canopy roughness length for momentum (m), z_{0H} is the canopy roughness length for heat (m), and k is the Von Karman constant (≈0.41). The displacement height and the canopy roughness lengths are estimated by simplified expressions as functions of canopy height, h (m): $d = 2h/3$, $z_{0M} = h/10$, and z_{0H} is taken as a fraction of z_{0M} ($z_{0H} = z_{0M}/7$). The stability functions for heat, Ψ_H, and for momentum, Ψ_M, are obtained from Brutsaert (1999):

$$\Psi_M(y) = Ln(a + y) - 3by^{1/3} + \frac{ba^{1/3}}{2} Ln\left[\frac{(1 + x)^2}{(1 - x + x^2)}\right] + 3^{1/2}ba^{1/3}\tan^{-1}[(2x - 1)/3^{1/2}] + \Psi_0 \quad \text{(unstable conditions)} \quad \text{(A4)}$$

$$\Psi_H(y) = [(1 - d)/n]Ln[(c + y^n)/c] \quad \text{(unstable conditions)} \quad \text{(A5)}$$

$$\Psi_M(y) = \Psi_H(y) = 5y \quad \text{(stable conditions)} \quad \text{(A6)}$$

in which $x = (y/a)^{1/3}$, and $y = -(z - d)/L$. The symbol Ψ_0 denotes a constant of integration, given by $\Psi_0 = (-Ln(a) + 3^{1/2}ba^{1/3}\pi/6)$. The parameters a, b, c, d, and n are assigned constant values of 0.33, 0.41, 0.33, 0.057, and 0.78, respectively (Brutsaert, 1999). L is the Monin-Obukhov length (m) and is expressed as

$$L = \frac{-u*^3\rho}{kg[(H/T_aC_p) + 0.61E]} \quad \text{(A7)}$$

where u^* is the friction velocity, ρ is the air density (kg m^{-3}), g is the acceleration of gravity (m s^{-2}), C_p is the air specific heat at constant pressure (J kg^{-1} K^{-1}), H is the sensible heat flux, and E is the rate of surface evaporation (kg m^{-2} s^{-1}). Neutral conditions are firstly assumed, and the initial estimations of H and LE are used to obtain an initial value of L. An iteration process is then applied until convergence.

u_s is the wind speed at height above the soil surface where the effect of soil surface roughness on the free wind movement can be neglected, z' (m s^{-1}) (Sauer et al., 1995). This wind speed is determined assuming a logarithmic wind profile in the air space above the soil:

$$u_s = u\left[\frac{Ln(z'/z'_0)}{Ln(z_u/z'_0) - \Psi_M}\right] \quad \text{(A8)}$$

where z'_0 is the soil roughness length (roughness length of the understorey vegetation has been considered in this case to account for the difference with a bare soil surface).

The effective surface emissivity is obtained from Valor and Caselles (1996):

$$\varepsilon = \varepsilon_c P_v(\theta) + \varepsilon_s(1 - P_v(\theta))(1 - 1.74P_v(\theta)) + 1.7372P_v(\theta)(1 - P_v(\theta))) \quad \text{(A9)}$$

The angular vegetation cover fraction $P_v(\theta)$ can be estimated assuming a spherical leaf angle distribution, via:

$$P_v(\theta) = 1 - \exp\left(\frac{-0.5\Omega(\theta)LAI}{\cos(\theta)}\right) \quad \text{(A10)}$$

where $\Omega(\theta)$ is a clumping factor to characterize the statistical distribution of phytoelements (Anderson et al., 2005). The clumping factor typically varies with the viewing angle, attaining a minimum value at nadir view (Ω_0). An empirical expression can be used to determine Ω_0 from the *LAI* value: $\Omega_0 = 0.492[1 + \exp(-0.52(\text{LAI}-0.45))]$ (Chen, 1996).

REFERENCES

Anderson, M.C., Norman, J.M., Kustas, W.P., Li, F., Prueger, J.H., Mecikalski, J.R., 2005. Effects of vegetation clumping on two-source model predictions of surface energy fluxes from an agricultural landscape during SMACEX. Journal of Hydrometeorology 6, 892–909.

Aurela, M., Laurila, T., Tuovinen, J.P., 2001. Seasonal CO_2 balances of a subartic mire. Journal of Geophysical Research 106, 1623–1638.

Baldocchi, D.D., Vogel, C.A., 1996. A comparative study of water vapor, energy and CO_2 flux densities above and below a temperate broadleaf and a boreal pine forest. Tree Physiology 16, 5–16.

Baldocchi, D., 2003. Assessing the eddy covariance technique for evaluating carbon dioxide exchange rates of ecosystems: past, present and future. Global Change Biology 9, 479–492.

Baldocchi, D.D., Vogel, C.A., Hall, B., 1997. Seasonal variation of energy and water vapour exchange rates above and below a boreal jack pine forest canopy. Journal of Geophysical Research 102 (D24), 28939–28951.

Berk, A., Anderson, G.P., Acharya, P.K., Chetwynd, J.H., Bernstein, L.S., Shettle, E.P., Matthew, M.W., Adler-Golden, S.M., 1999. MODTRAN 4 User's Manual. Air Force Research Laboratory, Space Vehicles Directorate, Air Force Materiel Command, Hascom AFB, MA.

Brutsaert, W., 1982. Evaporation into The Atmosphere. D. Reidel, Dordrecht, 299 pp.

Brutsaert, W., 1999. Aspects of bulk atmospheric boundary layer similarity under free-convective conditions. Reviews of Geophysics 37 (4), 439–451.

Chachine, M.T., Aumann, H., Goldberg, M., Mcmilin, L., Roserkranz, P., Staelin, D., Strow, L., Sussking, J., 2001. AIRS-Team Retrieval for Core Products and Geophysical Parameters. ATBD, 198 pp.

Chen, J.M., 1996. Optically-based methods for measuring seasonal variation of leaf area index in boreal conifer stands. Agricultural and Forest Meteorology 80, 135–163.

Choudhury, B.J., Idso, S.B., Reginato, R.J., 1987. Analysis of an empirical model for soil heat flux under a growing wheat crop for estimating evaporation by an infrared-temperature based energy balance equation. Agricultural and Forest Meteorology 39, 283–297.

Davidson, M., Moya, I., Ounis, A., Louis, J., Ducret, J.M., Moreno, J., Caselles, V., Sobrino, J.A., Alonso, J., Pedrós, R., Jiménez, J.C., Gómez-Amo, J.L., Soria, G., Niclòs, R., El-Kharraz, J., Martínez, J.A., Utrillas, M.A., Miller, Laurila, T., Thurn, T., 2002. The solar induced fluorescence experiment (SIFLEX-2002): campaign overview. In: Proceedings of FLEX Workshop, ESA SP-527, Noodwijk, Holland.

Finnigan, J., 2006. The storage term in eddy flux calculations. Agricultural and Forest Meteorology 136, 108–113.

Foken, T., Wimmer, F., Mauder, M., Thomas, C., Liebethal, C., 2006. Some aspects of the energy balance closure problem. Atmosphere Chemistry Physics 6, 4395–4402.

François, C., 2002. The potential of directional radiometric temperatures for monitoring soil and leaf temperature and soil moisture status. Remote Sensing of Environment 80, 122–133.

Grant, R.F., Zhang, Y., Yuan, F., Wang, S., Hanson, P.J., Gaumont-Guay, D., Chen, J., Black, T.A., Barr, A., Baldocchi, D.D., Arain, A., 2006. Intercomparison of techniques to model water stress effects on CO_2 and energy exchange in temperate and boreal deciduous forests. Ecological Modelling 196, 289–312.

Gu, L.H., Meyers, T., Pallardy, S.G., Hanson, P.J., Yang, B., Heuer, M., Hosman, K.P., Liu, Q., Riggs, J.S., Sluss, D., Wullschleger, S.D., 2007. Influences of biomass heat and biochemical energy storages on the land surface fluxes and radiative temperature. Journal of Geophysical Research-Atmospheres 112 (D2), D02107.

Gustafsson, D., Lewan, E., van der Hurk, B.J.J.M., Viterbo, P., Grelle, A., Lindroth, A., Cienciala, E., Mölder, M., Halldin, S., Lundin, L.-C., 2003. Boreal forest surface parameterization in the ECMWF Model-1D Test with NOPEX long-term data. Journal of Applied Meteorology 42, 95–112.

Haverd, V., Cuntz, M., Leuning, R., Keith, Heather, 2007. Air and biomass heat storage fluxes in a forest canopy: calculation within a soil vegetation atmosphere transfer model. Agricultural and Forest Meteorology 147, 125–139.

Humes, K.S., Kustas, W.P., Moran, M.S., 1994. Use of remote sensing and reference site measurements to estimate instantaneous surface energy balance components over a semiarid rangeland watershed. Water Resources Research 30, 1363–1373.

Jia, L., Li, Z.-L., Menenti, M., Su, Z., Verhoef, W., Wan, Z., 2003. A practical algorithm to infer soil and foliage component temperatures from biangular ATSR-2 data. International Journal of Remote Sensing 24 (23), 4739–4760.

Kustas, W.P., Goodrich, D.C., 1994. Preface. Water Resources Research 30, 1211–1225.

Kustas, W.P., Daughtry, C.S.T., van Oevelen, P.J., 1993. Analytical treatment of the relationships between soil flux/net radiation ratio and vegetation indices. Remote Sensing of Environment 46, 319–330.

Lamaud, E., Brunet, Y., Berbigier, P., 1996. Radiation and water use efficiencies of two coniferous forest canopies. Physical Chemistry of the Earth 21, 361–365.

Lamaud, E., Ogée, J., Brunet, Y., Berbigier, P., 2001. Validation of eddy flux measurements above the understorey of a pine forest. Agricultural and Forest Meteorology 106, 187–203.

Lafreur, P.M., 1992. Energy balance and evapotranspiration from a subartic forest. Agricultural and Forest Meteorology 58, 163–175.

Legrand, M., Pietras, C., Brogniez, G., Haeffelin, M., Abuhasan, N.K., Sicard, M., 2000. A high-accuracy multiwavelengh radiometer for in situ measurements in the thermal infrared. Part I. Characterization of the instrument. Journal of Atmospheric and Oceanic Technology 17, 1203–1214.

Li, F., Kustas, W.P., Prueger, J.H., Neale, C.M.U., Jackson, J.J., 2005. Utility of remote sensing based two-source energy balance model under low and high vegetation cover conditions. Journal of Hydrometeorology 6 (6), 878–891.

Lindroth, A., 1985. Seasonal and diurnal variation of energy budget components in coniferous forests. Journal of Hydrology 82, 1–15.

Massman, W.J., Lee, X., 2002. Eddy covariance flux corrections and uncertainties in long-term studies of carbon and energy exchanges. Agricultural and Forest Meteorology 113, 121–144.

Merlin, O., Chehbouni, A., 2004. Different approaches in estimating heat flux using dual angle observations of radiative surface temperature. International Journal of Remote Sensing 25 (1), 275–289.

McCaughey, J.H., 1985. Energy balance storage terms in a mature mixed forest at Petawawa, Ontario—a case study. Boundary Layer Meteorology 31, 89–101.

Moran, M.S., Humes, K.S., Printer, P.J., 1997. The scaling characteristics of remotely-sensed variables for sparsely-vegetated heterogeneous landscapes. Journal of Hydrology 190, 337–362.

Niclòs, R., Caselles, V., Coll, C., Valor, E., Sánchez, J.M., 2005. In situ surface temperature retrieval in a boreal forest under variable cloudiness conditions. International Journal of Remote Sensing 26 (18), 3985–4000.

Njoku, E.G., Hook, S.J., Chehbouni, A., 1996. Effects of surface heterogeneity on thermal remote sensing of land parameters. In: Stewart, J.B., Engman, E.T., Feddes, R.A., Kerr, Y. (Eds.), Scaling Up in Hydrology Using Remote Sensing. John Wiley & Sons, West Sussex, UK, Chapter 2, pp. 19–31.

Norman, J.M., Kustas, W., Humes, K., 1995. A two-source approach for estimating soil and vegetation energy fluxes from observations of directional radiometric surface temperature. Agricultural and Forest Meteorology 77, 263–293.

Oliphant, A.J., Grimmond, C.S.B., Zutter, H.N., Schmid, H.P., Su, H.-B., Scott, S.L., Offerle, B., Randolph, J.C., Ehman, J., 2004. Heat storage and energy balance fluxes for a temperate deciduous forest. Agricultural and Forest Meteorology 126, 185–201.

Ogawa, K., Schmugge, T., Jacob, F., French, A., 2002. Estimation of broadband land surface emissivity from multi-spectral thermal infrared remote sensing. Agronomie 22, 695–696.

Rubio, E., Caselles, V., Badenas, C., 1997. Emissivity measurements of several soils and vegetation types in the 8–14 μm wave band: analysis of two fields methods. Remote Sensing of Environment 59, 490–521.

Rubio, E., Caselles, V., Coll, C., Valor, E., Sospedra, F., 2003. Termal-infrared emissivities of natural surfaces: improvements on the experimental set-up and new measurements. International Journal of Remote Sensing 24, 5379–5390.

Russell, M.J., Núñez, M., Chladil, M.A., Valiente, J.A., López Baeza, E., 1997. Conversion of nadir, narrowband reflectance in red and near-infrared channels to hemispherical surface albedo. Remote Sensing of Environment 61, 16–23.

Salisbury, J.W., D'Aria, D.M., 1992. Emissivity of terrestrial materials in the 8–14 μm atmospheric window. Remote Sensing of Environment 42, 83–106.

Sánchez, J.M., Caselles, V., Niclòs, R., Valor, E., Coll, C., Laurila, T., 2007. Evaluation of the B-method for determining actual evapotranspiration in a boreal forest from MODIS data. International Journal of Remote Sensing 28 (5–6), 1231–1250.

Sánchez, J.M., Kustas, W.P., Caselles, V., Anderson, M.C., 2008a. Modelling surface energy fluxes over maize using a two-source patch model and radiometric soil and canopy temperature observations. Remote Sensing of Environment 112, 1130–1143.

Sánchez, J.M., Scavone, G., Caselles, V., Valor, E., Copertino, V.A., Telesca, V., 2008b. Monitoring daily evapotranspiration at a regional scale from Landsat-TM and ETM + data: application to the Basilicata region. Journal of Hydrology 351, 58–70.

Santanello, J.A., Friedl, M.A., 2003. Diurnal covariation in soil heat flux and net radiation. Journal of Applied Meteorology 42, 851–862.

Sauer, T.J., Norman, J.M., Tanner, C.B., Wilson, T.B., 1995. Measurement of heat and vapour transfer coefficients at the soil surface beneath a maize canopy using source plates. Agricultural and Forest Meteorology 75, 161–189.

Sellers, P.J., Hall, F., Margolis, H., Kelly, B., Baldocchi, D., den Hartog, G., Cihlar, J., Ryan, M.G., Goodison, B., Crill, P., Ranson, K.J., Lettenmaier, D., Wickland, D.E., 1995. Boreal Ecosystem-Atmosphere Study (BOREAS): an overview and early results from the 1994 field year. Bulletin of American Meteorological Society 76, 1549–1577.

Sellers, P.J., Hall, F.G., Kelly, R.D., Black, A., Baldocchi, D., Berry, J., Ryan, M., Ranson, K.J., Crill, P.M., Lettenmaier, D.P., Margolis, H., Cihlar, J., Newcomer, J., Fitzjarrald, D., Jarvis, P.G., Gower, S.T., Halliwell, D., Williams, D., Goodison, B., Wickland, D.E., Guertin, F.E., 1997. BOREAS in 1997: experiment overview, scientific results and future directions. Journal of Geophysical Research 102 (D24), 28731–28770.

Shuttleworth, W.J., 1989. Micrometeorology of temperate and tropical forests. Philosophical Transactions of the Royal Society of London, Series B 324, 299–334.

Snyder, W.C., Wan, Z., Zhang, Y., Feng, Y., 1997. Thermal infrared (3–14 μm) bi-directional reflectance measurements of sands and soils. Remote Sensing of Environment 60, 101–109.

Stannard, D.I., Blanford, J.H., Kustas, W.P., Nichols, W.D., Amer, S.A., Schmugge, T.J., Weltz, M.A., 1994. Interpretation of surface flux measurements in heterogeneous terrain during the Monsoon' 90 experiment. Water Resources Research 30 (5), 1227–1239.

Twine, T.E., Kustas, W.P., Norman, J.M., Cook, D.R., Houser, P.R., Meyers, T.P., Prueger, J.H., Starks, P.J., Wesely, M.L., 2000. Correcting eddy-covariance flux underestimates over a grassland. Agricultural and Forest Meteorology 103 (3), 279–300.

Valor, E., Caselles, V., 1996. Mapping land surface emissivity from NDVI. Application to European, African and South-American areas. Remote Sensing of Environment 57, 167–184.

Wilson, K., Goldstein, A., Falge, E., Aubinet, M., Baldocchi, D., Berbigier, P., Bernhofer, C., Ceulemans, R., Dolman, H., Field, C., Grelle, A., Ibrom, A., Law, B.E., Kowalski, A., Meyers, T., Moncrieff, J., Monson, R., Oechel, W., Tenhunen, J., Valentini, R., Verma, S., 2002. Energy balance closure at FLUXNET sites. Agricultural and Forest Meteorology 113, 223–243.

Wu, A., Black, A., Verseghy, D.L., Bailey, W.G., 2001. Comparison of two-layer and single-layer canopy models with lagrangian and k-theory approaches in modelling evaporation from forests. International Journal of Climatology 21, 1821–1839.

Zhan, X., Kustas, W.P., Humes, K.S., 1996. An intercomparison study on models of sensible heat flux over partial canopy surfaces with remotely sensed surface temperature. Remote Sensing of Environment 58, 242–256.